Paper

BREATH BIOMARKERS OF WHOLE-BODY GAMMA IRRADIATION IN THE GÖTTINGEN MINIPIG

Michael Phillips,*† Renee N. Cataneo,* Anirudh Chaturvedi,* Peter D. Kaplan,* Mark Libardoni,‡ Mayur Mundada,* Urvish Patel,* Karla D. Thrall,§ and Xiang Zhang**

Abstract—**There is widespread interest in the development of tools to estimate radiation exposures. Exhaled breath provides a novel matrix for assessing biomarkers that could be correlated with exposures. The use of exhaled breath for estimating radiation exposure is warranted, as studies have shown that external exposure to ionizing radiation causes oxidative stress that accelerates lipid peroxidation of polyunsaturated fatty acids, liberating alkanes and alkane metabolites that are excreted in the breath as volatile organic compounds (VOCs). As a proof of principle study, small groups (n = 4) of Göttingen minipigs were whole-body irradiated with gamma rays delivered by a ^{60}Co source at absorbed doses of 0, 0.25, 0.5, 0.75, 1, 1.25, 2, and 4 Gy. Additional groups (n = 4) were treated with lipopolysaccharide (LPS) or granulocyte colony stimulating factor (G-CSF), with and without concurrent ^{60}Co exposure, at an absorbed dose of 1 Gy. Breath and background air VOC samples were collected on days −3, −2, −1, 0 pre-irradiation, then at 0.25, 24, 48, 72, and 168 h post-irradiation. VOCs were analyzed by automated thermal desorption with two-dimensional gas chromatography and time-of-flight mass spectrometry (ATD GCxGC TOF MS). The results show significant changes in 58 breath VOCs post-irradiation, mainly consisting of methylated and other derivatives of alkanes, alkenes, and benzene. Using a multivariate combination of these VOCs, a radiation response function was constructed, which was significantly elevated at 15 min post irradiation and remained elevated throughout the study (to 168 h post irradiation). As a binary test of radiation absorbed doses ≥ 0.25 Gy, the radiation response function distinguished irradiated animals from shams (0 Gy) with 83–84% accuracy. A randomly derived radiation response function was robust: When half of the biomarkers were removed, accuracy was 75%. An optimally derived function with two biomarkers was 82% accurate. As a binary test of radiation absorbed doses ≥ 0.5 Gy, the radiation response function identified irradiated animals with an accuracy of 87% at 15 min post irradiation and 75.5% at 168 h post irradiation. Treatment with LPS and G-CSF did not affect the radiation response function. This proof-of-principle study supports the hypothesis that breath VOCs may be used for estimating radiation exposures. Further studies will be required to validate the sensitivity and specificity of these potential biomarkers. Health Phys. 108(5):538–546; 2015**

Key words: exposure, radiation; radiation dose; radiation effects; radiation, biology

INTRODUCTION

Recent concerns over nuclear accidents and threats of terrorism have spurred efforts to develop rapid methods for screening individuals for assessing exposures to ionizing radiation. These methods are generally termed radiation biodosimetry, which is the use of physiological, chemical, or biological markers of exposure of human tissues to ionizing radiation for the purpose of reconstructing doses to individuals or populations (NCRP 2009). A number of different techniques have been reported for radiation biodosimetry, including detection of induced chromosomal abnormalities (Wilkins et al. 2008; Moroni et al. 2010) and electron paramagnetic resonance in teeth. Signatures of radiation exposure in blood include various approaches to gene expression (Chaudhry 2008) and protein phosphorylation patterns (Marchetti et al. 2006) or lymphocyte suppression (Moroni et al. 2011). However, there is a general consensus that a richer set of biological measures is necessary, as each mode of response has its own particular benefits and limitations (Pass 1997).

This laboratory has been investigating a noninvasive biomonitoring approach focused on measurement of volatile organic compounds (VOCs) in exhaled breath to estimate external radiation exposures. Previous studies have shown that radiation-induced oxidative stress can generate specific VOCs that are excreted in exhaled breath as metabolic products (Arterbery et al. 1994). Ionizing radiation oxidizes water, resulting in the generation of hydroxyl radicals and reactive

*Breath Research Laboratory, Menssana Research Inc, 211 Warren St, Newark, NJ 07103; †Department of Medicine, New York Medical College, Valhalla, NY; ‡Southwest Research Institute, 6220 Culebra Rd, San Antonio, TX 78238; §Pacific Northwest National Laboratory, 902 Battelle Boulevard, Richland, WA 99352; **Department of Chemistry, University of Louisville, 2320 South Brook Street, Louisville, KY 40292.

The authors declare no conflicts of interest.

For correspondence contact: Michael Phillips Breath Research Laboratory, Menssana Research Inc, 211 Warren St, Newark, NJ 07103, or email at **mphillips@menssanaresearch.com**.

(*Manuscript accepted* 11 *December* 2014)
0017-9078/15/0

DOI: 10.1097/HP.0000000000000272

oxygen species (ROS) that cause oxidative stress (Riley 1994). ROS accelerates lipid peroxidation of polyunsaturated fatty acids in cell membranes, liberating alkanes and alkane metabolites that are excreted in the breath due to their high vapor pressure at body temperature (Kneepkens et al. 1994). Additionally, a number of studies have shown that irradiation of animal and plant tissues in foodstuffs elicits production of several different VOCs, including alkanes and alkenes consistent with oxidative stress products (Barba et al. 2012; Nam et al. 2011) as well as benzene derivatives and aldehydes of undefined metabolic source (Zhu et al. 2004; Ismail et al. 2009). Development of a noninvasive, painless, and safe breath test for biomarkers indicative of external radiation exposure offers considerable convenience over tests employing blood or other body fluids.

The study reported here is a proof-of-principle study focused on the utility of volatile biomarkers in exhaled breath of whole-body gamma irradiated Göttingen minipigs. The Göttingen minipig has gained popularity among the research community due to its convenience in handling, small size, well-characterized genotype, and the close sequence homology between swine and humans (Forster et al. 2010). A breath collection apparatus (BCA) was used to capture VOCs from minipig exhaled breath onto sorbent tubes, which then underwent a comprehensive analysis using two-dimensional gas chromatography time-of-flight mass spectrometry (GCxGC TOF MS).

MATERIALS AND METHODS

Animals

Sixty-five male Göttingen minipigs (ages 3–5 mo, average body weight approximately 10 kg at time of irradiation) were obtained from Marshall BioResources (North Rose, NY) and randomly distributed to groups of four animals each. Animals were housed individually in modular floor pens measuring 1.1 m^2. Pens were attached in units, allowing pigs to see and touch neighboring animals. Autoclaved aspen wood shavings were provided for bedding and were changed at least daily. Individual water lines with lixit valves were secured to pen walls; polyethylene balls (Bio-Serv, Frenchtown, NJ) were provided for enrichment. Animals were fed Lab Diet K599 Certified Lab Minipig Grower and Maintenance feed (PMI Nutrition International, LLC, Brentwood, MO) in a ration based on age twice daily. Certified fruit crunchies (Bio-Serv, Frenchtown, NJ) and locally procured apples and miniature marshmallows were used for positive reinforcement. The light cycle was 12 h light and 12 h dark, and temperature and humidity were as recommended for minipigs provided bedding: 18−22°C and 35−65% humidity, respectively. Animals were allowed to acclimate fully to the facility for at least 2 wk prior to irradiation. Temperature and identification transponders were implanted subcutaneously (BMDS IPTT-300, Seaford, DE) during the acclimation period. The Institutional Animal Care and Use Committee at Battelle, Pacific Northwest Division, approved animal protocols.

Irradiation procedure

Animals were whole-body irradiated with gamma rays (1,170 and 1,330 keV) delivered by a ^{60}Co source. The absorbed dose rate was 0.39 Gy min^{-1}, and absorbed doses of 0.5 to 8 Gy were delivered in a single fraction. Radiation exposure and dosimetry followed recommendations set forth in Report 30 of the International Commission on Radiation Units and Measurements. Anesthetized animals were irradiated using a nominal 173,900 GBq ^{60}Co source contained within an automated irradiator. The source selected was moved into place using a pneumatic system to a position 170 cm above the floor within a collimator that provided an approximate 30-degree solid angle beam. Prior to irradiating live animals, the correlation between internal center-line dose measurements using LiF:Mg:Ti "chipstrate" dosimeters in a euthanized animal and external exposure using a Capintec ionization chamber were established. Two separate dosimetric methods were used, so results could be compared and uncertainties in the accuracy of the measured doses known to a high degree. Chipstrate dosimeters were calibrated in a National Institute of Standards and Technology (NIST)-traceable ^{60}Co beam using tissue-equivalent plastic for buildup to accommodate a reference to absorbed dose to tissues. Passive dosimeter and ionization chamber measurements showed the same (within 2%) absorbed dose rate at the center of the reference minipig. The accuracy of this dose relative to the national standard was estimated to be ± 7.5% at the 95% confidence level.

For irradiation, anesthetized animals were restrained in a hammock-style sling with legs positioned under the animal and placed on a rotating platform. A remotely operated platform turntable rotated the sling and restrained animal. To achieve the desired target dose rate of approximately 400 mGy min^{-1}, animals in slings were positioned approximately 90 cm from the source. Due to this close distance and the need to use continuous rotation during exposures, the outer edges of the gamma-ray beam were shaped using aluminum attenuators. This provided dose uniformity across the entire body. Whole body gamma-irradiation doses ranged from 0.25−2.0 Gy at a dose rate of approximately 400 mGy min^{-1}. Day of irradiation was considered day 0.

Breath sample collection

The method has been described in detail (Phillips et al. 2003). The breath collection apparatus (Menssana Research, Inc., Fort Lee, NJ) was interfaced with an anesthetic mask in order to collect samples from the animals. At each time point, exhaled breath was collected for 4 min at a rate of 0.5 L min^{-1}. Alveolar breath and ambient room air were

Table 1. ***Treatment groups***. Breath samples were collected from all animals at 24-h intervals during the baseline period of 4 d prior to irradiation and then following irradiation at 0.25, 24, 48, 72, and 168 h. G-CSF = granulocyte colony stimulating factor, LPS = lipopolysaccharide, and IR = irradiated. The sham animals were managed in the same fashion as animals in the irradiation and confounder groups, with the absence of radiation.

		Dose (Gy)	No. animals
Irradiation groups	Sham	0	8
	irradiated	0.5	4
		1	4
		1.5	4
		2	4
		2.5	4
		4	4
		8	4
Confounder groups	Sham	0	4
	0.9% saline	0	4
	IR	2	4
	LPS + IR	2	4
	G-CSF+IR	2	4
	LPS	0	4
	G-CSF	0	4

captured onto separate sorbent traps containing graphitized carbon black (Supelco Inc., Bellefonte, PA). Breath sampling occurred pre-irradiation days −3, −2, −1, 0, and then at 15 min, 24 h, 48 h, 72 h, and 168 h post-irradiation. Animals were acclimated to sling restraint for breath collections.

Effects of potential confounding factors

The effects of a single dose of lipopolysaccharide (LPS) and granulocyte colony stimulating factor (G-CSF) were studied with and without irradiation (Table 1). Animals in the G-CSF group received Neupogen (Amgen, NDC 5513-53-10, Lot #1022977) diluted to 30 μg mL^{-1} in 5% dextrose and administered intravenously at a dose of 5 μg kg^{-1}. Animals in the LPS group received LPS (Sigma L2880, Lot#110M4086V) diluted to 125 μg mL^{-1} in 0.9% saline and administered at a dose of 50 μg kg^{-1} by intraperitoneal injection.

Anesthesia and analgesia. Animals were anesthetized with ketamine (33 mg kg^{-1}) and acepromazine (1.1 mg kg^{-1}) by intramuscular (IM) injection. Analgesia (carprofen 2–3 mg kg^{-1} oral twice a day) was provided to each animal within 24 h following irradiation and continued for the duration of the study. For blood collection, animals were sedated using midazolam [0.1–0.5 mg kg^{-1} subcutaneous (SC) or IM] or acepromazine (1.1 mg kg^{-1} IM) for animals that were resistant to midazolam. At the completion of the study, animals were anesthetized with ketamine (33 mg kg^{-1}) and acepromazine (1.1 mg kg^{-1}) by IM injection and euthanized with sodium pentobarbital (150 mg kg^{-1}).

Analysis of samples

Breath and air samples captured on the sorbent traps were analyzed by automated thermal desorption (ATD) and two-dimensional gas chromatography with time-of-flight mass spectrometry (ATD GCxGC TOF MS). For ATD (Unity 2 thermal desorber; Markes International Inc., Cincinnati, OH, USA), water vapor was first purged from the sorbent traps with helium carrier gas, and then an internal standard of 2 ppm 1-bromo-4-fluoro-benzene (BFB; Supelco Inc., Bellefonte, PA) was injected onto each sorbent trap. The sorbent trap was then heated under 55 mL min^{-1} helium flow. Volatile compounds desorbed from the trap are captured and reconcentrated on a Peltier cooled cold trap. For the GCxGC, samples were transferred under helium flow onto the head of the primary column of the GCxGC TOF MS (Pegasus 4D with an Agilent 6890 gas chromatograph and a LECO two-stage cryogenic modulator and a secondary oven, LECO Corp., St. Joseph, MI). Two capillary columns (30 m relative non-polar primary column and 2 m more polar secondary column; Restek, Bellefonte, PA) were connected in series, separated by the cryogenic modulator with 5 s cycle time. The columns were heated using multiple temperature ramps from 35 to 280°C. The second column was held 20° C higher than the first. For TOF MS, 70 eV electrons ionized and fragmented material coming off the GC. Mass spectra were recorded at 2 kHz by the TOF MS over an m/z range of 35–400. This method was effective at separating the large number of VOCs detected in breath and room air.

Data treatment

Chromatographic data were processed using LECO's ChromaTof software for peak detection and compound identification. VOCs were identified by their mass spectral

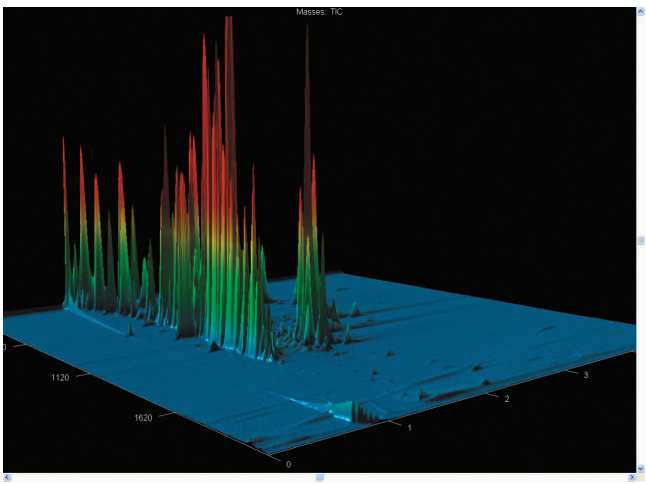

Fig. 1. Typical chromatogram of minipig breath VOCs: Breath VOC samples were analyzed using comprehensive two-dimensional gas chromatography time-of-flight mass spectrometry. Separation with non-polar and polar columns revealed around 700 different VOCs on average in a sample of minipig breath.

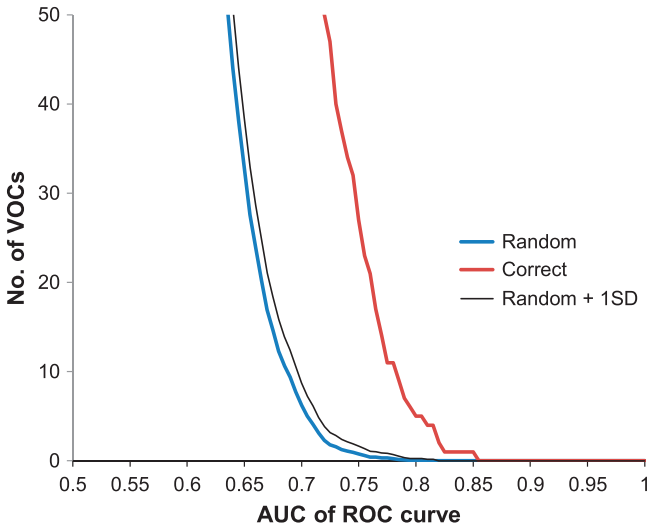

Fig. 2. Identification of biomarkers of radiation. *Monte Carlo simulations—shams vs. 0.5 Gy (upper panel).* Breath VOCs in irradiated animals and sham animals were compared with multiple Monte Carlo simulations. The criterion of the accuracy of a breath VOC as a biomarker of radiation exposure was the area under curve (AUC) of its receiver operating characteristic (ROC) curve, a value that ranges between 0.5 (no better than a random coin toss) and 1.0 (a perfect test with no false positive or false negative results). All VOCs in the sample are included when AUC = 0.5 and the number of VOCs progressively declines as the AUC threshold increases. The "correct assignment" curve shows the outcome when the subject was correctly assigned to the appropriate group (radiation or sham). The "random assignment" curve shows the mean outcome of 40 Monte Carlo simulations in which animals were randomly assigned to the radiation group or to the sham group. The number of VOCs in the mean random assignment curve fell to <1 when ROC curve AUC = 0.85. However, 32 breath VOCs in the correct assignment group had ROC curve AUC values >0.74, demonstrating that these VOCs identified radiation exposure with greater than random accuracy (>5 SD). *Overlap of biomarkers at different dosages of radiation (lower panel):* The Venn Diagram displays the extensive overlap between the outcomes of multiple Monte Carlo simulations at different dosages of radiation. A total of 58 VOCs was observed in at least one or more different dosages of radiation, and these were employed in the derivation of the radiation response function.

signatures matched to a mass spectral library (NIST 2.0, Gaithersburg, MD). After retention index filtering (Li et al. 2011), all peak lists were aligned using an improved version of DISCO software (Wang et al. 2010). Peaks with low quality were removed; multiple peak entities were merged using the default values specified in DISCO when spectral similarity was calculated (Kim et al. 2012) and used to align peaks between samples.

Determination of alveolar gradients

The value of the alveolar gradient for each breath VOC was determined as $V_b/l_b - V_a/l_a$ where V_b is the area under the curve (AUC) of the chromatographic peak of a VOC in breath; l_b is the AUC of the internal standard (BFB) peak in the same chromatogram; and V_a and l_a denote the corresponding values in the associated room air sample (Phillips et al. 2003).

Identification of biomarkers associated with external radiation exposure

The VOCs, whose abundance varied with external radiation exposure, were identified by checking the receiver operating characteristic (ROC) curve for each compound in the breath. The significance of each result was tested using multiple Monte Carlo simulations, which randomly permute the assignment of animals to exposure groups. This method has been previously described (Phillips et al. 2010). In summary, the alveolar gradients of all breath VOCs collected post irradiation exposure were compared between groups. The VOCs were then ranked as candidate biomarkers according to their C-statistic values; i.e., the AUC of the ROC curve (Cook 2008). The average random behavior of the alveolar gradients of all breath VOCs was determined with multiple Monte Carlo simulations that randomly permute the assignment of subjects to irradiated vs. sham (0 Gy) group and calculate the C-statistic value. C-statistic values for the correct assignments that exceed the largest average value observed across the 40 permutations of random assignment identify VOCs that exhibit greater than random accuracy. These become candidate biomarkers to use in the development of a radiation response function (Ma et al. 2006; Yang et al. 2006).

RESULTS

Identification of biomarkers associated with external radiation exposure

Fig. 1 displays a typical chromatogram of breath VOCs from a sham (0 Gy) Göttingen minipig. Fig. 2 (upper panel)

displays the outcomes of multiple Monte Carlo simulations comparing all shams (0 Gy; n = 12) to animals exposed to 0.25 Gy (n = 4) when the results from all post-irradiation samples were pooled. These simulations identified 32 VOCs as better-than-chance biomarkers of external radiation exposure when employing a five sigma criterion. Similar Monte Carlo simulations identified 14 candidate exhaled breath VOC biomarkers in animals exposed to 0.75 Gy, eight VOCs in animals exposed to 1.25 Gy, 15 VOCs in animals exposed to 2 Gy, and eight VOCs in animals exposed to 4 Gy. The overlap in the identities of these VOC biomarkers is shown in Fig. 2 (lower panel). These VOCs mainly comprised methylated and other derivatives of alkanes, alkenes, and benzene. However, they could only be identified tentatively because of the potential confounding factors that may compromise identification of unknown compounds with the NIST library (Stein 2012).

Effects of anesthesia

Several breath VOCs were found to be significantly increased in exhaled breath collected from sham (0 Gy)-exposed animals when compared before and after administration of anesthesia. The potential confounding effects of anesthesia were controlled by ignoring these VOCs in post-irradiation exhaled breath samples from animals exposed to ^{60}Co.

Derivation of radiation response function

The intensity of the analytical detector response for candidate biomarker VOCs was correlated with levels of exposure to ^{60}Co using multivariate linear regression on the abundances, the abundances squared, and the abundances cubed (mvregress, MATLAB R2012a; Mathworks, Natick, MA, USA) employing chromatograms from all post-exposure animals except those in the confounder sets (LPS and GCSF). The response function was constructed from a dimensionless matrix A whose n rows represented individual breath samples and whose m columns contain the abundance of individual compounds. The abundance is the instrument peak area divided by the peak area of the internal standard, bromofluorbenzene for that chromatogram. To include nonlinear terms, an $n \times 3$ m matrix $\tilde{A}$ was constructed ($\tilde{A}_{ij}=A_{ik}^{p}$) where $k = mod(j,m)$ and $p = 1 + \text{floor}(j/m)$. Prior to fitting, each column of $\tilde{A}$ was zero centered and normalized by its variance. The vector of coefficients to estimate a radiation response function, β, was then calculated by regressing $\tilde{A}$ against the dosage D_i for chromatogram i, $\beta = \text{mvregress}(\tilde{A}, D)$. The resulting fit was then used to generate a single value for each chromatogram termed the "radiation response function" $R = \tilde{A}\ \beta$. The time course of the radiation response function is shown in Fig. 3 in all irradiated animals, including sham (0 Gy)-exposed animals (upper panel); the lower panel shows the same data stratified by ^{60}Co exposure levels.

Radiation biodosimetry

Fig. 4 displays the radiation response function in different groups of animals by ^{60}Co absorbed dose (top left panel) and the receiver operating characteristic (ROC) curves stratified by exposure level (top right panel) and by time post irradiation exposure (bottom left panel).

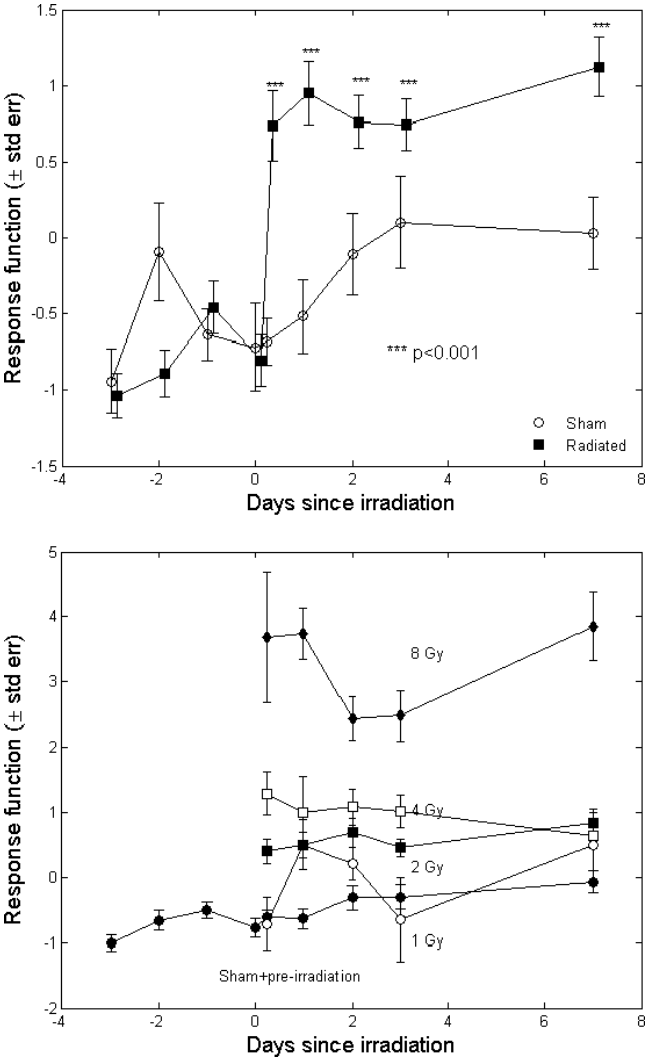

Fig. 3. Time course of breath test response to radiation. The radiation response function was derived from the significant biomarkers of radiation that were observed in at least two or more different dosages of radiation. Variation in the radiation response function is shown during the baseline period of four days prior to irradiation and then following irradiation at 15 min and 24, 48, 72, and 168 h. Each point displays the mean radiation response function and the standard error of the mean. *Upper panel: Radiation response function in all irradiated animals and sham animals.* The radiation response function was significantly elevated in irradiated animals at all time points following irradiation ($p < 0.001$). *Lower panel: Effect of dosage of radiation.* Data shown in the upper panel was stratified by dosage of radiation. The radiation response function was apparently elevated with increasing dosage.

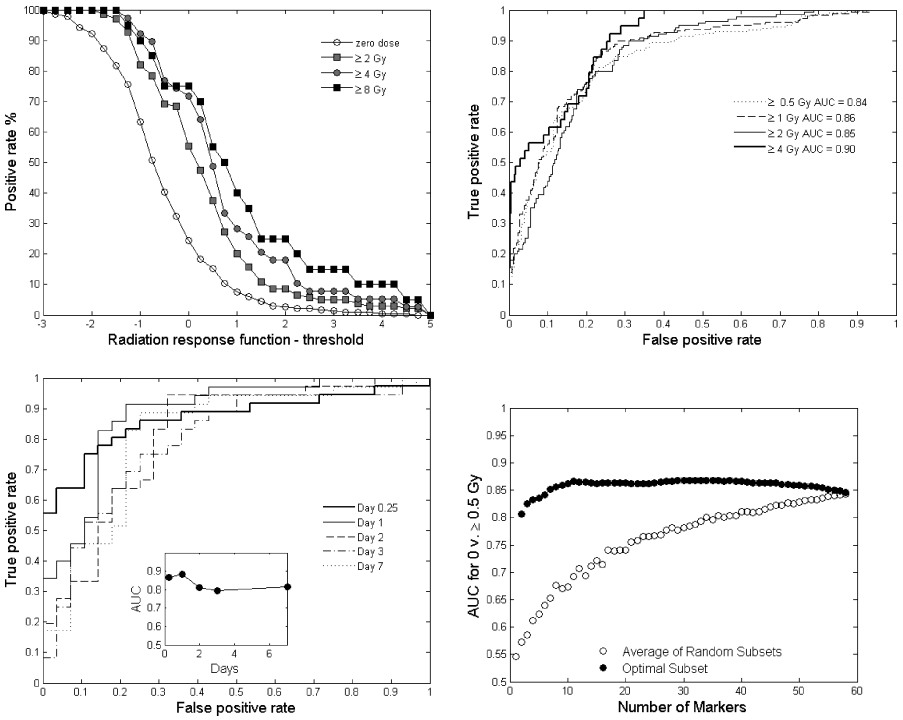

Fig. 4. Radiation biodosimetry. (1) *Radiation response function in different dosage groups (top left panel).* The radiation response function was ≥ −2 in all animals. Increases in the threshold value of the radiation response function distinguished animals in different dosage groups; e.g., when threshold = 2.0, the breath test was positive in 8% of animals receiving zero dosage of radiation compared to 18% at 2 Gy, 27% at ≥ 4Gy, and 40% at ≥ 8Gy. *Receiver operating characteristic (ROC) curves stratified by dosage of radiation (top right panel)*. The ROC curve displays variation in the true-positive rate (sensitivity) as a function of the false-positive rate (1-specificity). The area under curve (AUC) of the ROC curve indicates the overall accuracy of the breath test, ranging from 0.5 (no better than a random coin toss) to 1.0 (a perfect test with no false-positive or false-positive results). At all dosages from ≥0.5 Gy to ≥4 Gy, the breath radiation response function distinguished irradiated animals from shams with 83% − 84% accuracy. (2) *ROC curves stratified by time after irradiation (bottom left panel)*. The breath radiation response function distinguished irradiated animals from shams on all four days of the study at a cutoff value of 1 Gy. As shown in the inset, accuracy varied from 87 % on day 0 to 76 % on day 7. (3) *Robustness of the radiation response function (bottom right panel)*. Random subsets (open circles) display the average AUC of the ROC curve for detecting ≥ 0.5 Gy radiation as a function of number of biomarkers in the model. The AUC value was recalculated using randomly chosen subsets of the 58 candidate biomarkers and plotting the average AUC. Optimal subsets (closed circles) display the average AUC of this ROC curve by starting with the most significant of the 58 biomarkers and progressively adding one biomarker at a time. An optimally derived model containing only two biomarkers was an accurate binary indicator of radiation exposure (AUC = 0.83).

Robustness of the radiation response function

The AUC of the ROC curve for detecting differences between samples collected from animals exposed to ^{60}Co ≥ 0.25 Gy vs. sham (0 Gy) animals (Fig. 4, bottom right panel) was recalculated using randomly chosen subsets of the 58 candidate VOC biomarkers and plotting the average AUC as a function of the number of biomarkers in the model (open circles). Additionally, the average AUC of this ROC curve was determined by starting with the most significant of the 58 biomarkers and progressively adding one biomarker at a time in decreasing order of significance (closed circles). This figure shows that an optimally derived model may perform as an accurate binary indicator of external ^{60}Co exposure with as few as two biomarkers.

Effects of potential confounding factors

Fig. 5 shows the variation in the radiation response function over time in sham (0 Gy) animals and the effects of 0.9% saline, G-CSF, and LPS with and without confounding exposure to ^{60}Co. The G-CSF and LPS plus ^{60}Co-exposure groups consistently exhibited higher responses from 0.25 to 168 h post irradiation compared to non-irradiated (sham 0 Gy) animals treated with the same potential confounders.

DISCUSSION

The primary finding of this study was that single, whole-body ^{60}Co exposure altered the composition of volatile biomarkers in the exhaled breath of Göttingen minipigs. These changes were highly significant in that irradiation exposure increased or decreased the abundance of breath VOCs by more than five standard deviations in excess of variation arising by chance; this corresponds to a *p*-value of less than 10^{-6}. A radiation response function that combined the main biomarkers was significantly increased

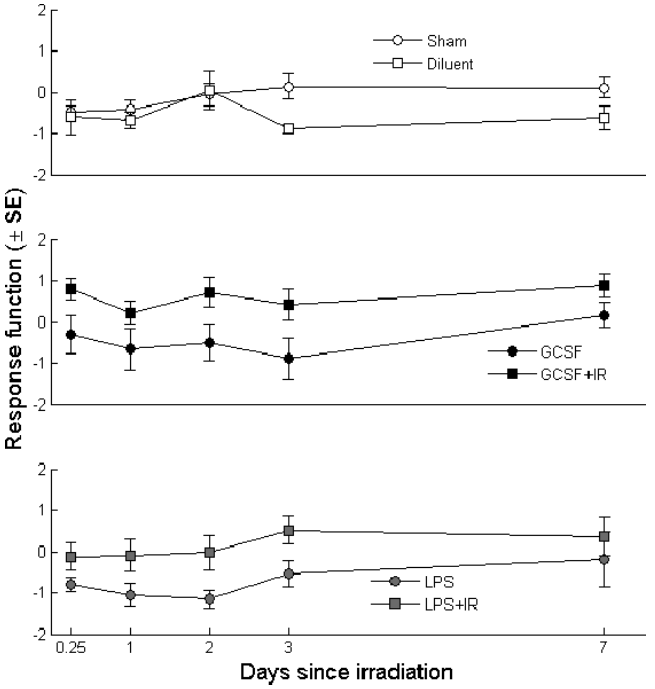

Fig. 5. Effects of potential confounding factors. Variation in the radiation response function over time is shown for sham animals and those receiving diluent (0.9% saline) (upper panel), animals treated with granulocyte colony stimulating factor (G-CSF) with and without irradiation (IR) (middle panel), and animals treated with lipopolysaccharide (LPS) with and without IR (lower panel).

within 15 min post-irradiation, and this increase persisted for the duration of the study period (7 d post irradiation; Fig. 3).

The majority of the volatile biomarkers associated with ^{60}Co exposure were comprised of methylated and other derivatives of alkanes, alkenes, and benzene. This finding was consistent with several previous reports of volatile products induced by irradiation of animal tissues, and they may have an origin, in part, from the effects of oxidative stress (Zhu et al. 2004; Ismail et al. 2009; Nam et al. 2011; Barba et al. 2012; Crohns et al. 2009; Guerrero et al. 2012; Fedrigo et al. 2010).

These findings support the potential value of exhaled breath testing as a candidate new tool for estimating external radiation exposures. The value of the multivariate radiation response function increased with absorbed dose of radiation (Fig. 4a). To demonstrate this point, the authors constructed binary responses using the radiation response function to identify irradiated animals at absorbed doses from ≥ 0.25 Gy to ≥ 2 Gy with 83–84% accuracy (Fig. 4b). At a cutoff value of 0.5 Gy, the breath radiation response function identified irradiated animals on all seven doses of the study with accuracy varying from 87% at 15 min post irradiation to 75.5% at 7 d post irradiation (Fig. 4c).

As in any biomarker discovery project, there is concern for false discovery as well as false non-discovery of markers. It was clear that no single VOC employed alone provided a useful biomarker. This may be because of individual variations between animals or other factors. The radiation response function, as a multivariate combination of multiple compounds, is comprised of signals from individual compounds that are present in some animals and not others and also at some doses and not others. For this reason, the robustness of the polynomial response function was tested by recalculating its accuracy using randomly selected subsets of the 58 biomarkers to identify absorbed doses ≥ 0.25 Gy. As shown in Fig. 4 (bottom right panel, open circles), the average accuracy of the polynomial response function (i.e., the AUC of the ROC curve) increased from 0.55 to 0.84 as breath biomarkers were added to the model. This figure illustrates that the polynomial response function was a robust indicator of radiation exposure because the average accuracy was comparatively insensitive to the addition or subtraction of biomarkers. Even when half of the biomarkers were discarded, the breath test delivered strong diagnostic accuracy (AUC > 0.75). This degree of robustness supports the main conclusion of the study—that a set of breath-based VOCs may be diagnostic in estimating external radiation exposure. An interesting corollary finding was that a polynomial response function could provide an accurate binary indicator of exposure with as few as two optimally selected biomarkers (Fig. 4, bottom right panel, closed circles).

The technique of breath collection and analysis is robust; previous studies reported that samples are stable at room temperature for at least five weeks, without degradation by loss of VOCs. The method is user-friendly, and operators can be trained rapidly to collect samples that are technically satisfactory. However, the comparatively small number of animals studied in this pilot project did not permit estimation of inter- and intra-animal variation of breath VOCs.

Two potential test confounders, LPS and G-CSF, did not affect the radiation response function (Fig. 5). The specificity of the radiation response signal, demonstrated by the insensitivity to confounders, could enhance the clinical value of a breath-based tool for evaluating casualties of a nuclear event. LPS is a Gram-negative bacterial endotoxin that causes septic shock (Rosenfeld and Shai 2006), a syndrome that mimics acute radiation toxicity. Nausea, diarrhea, vomiting, and fever may occur in both conditions. Consequently, it is desirable that a biomarker for estimating external radiation exposures should not respond to LPS in order to avert false-positive signals of radiation toxicity in persons suffering from septic shock. Similarly, it is desirable that a biomarker for estimating external radiation exposures should not respond to G-CSF, because this drug may be employed to treat acute radiation sickness (Li et al. 2011; Viswanath et al. 2008).

CONCLUSION

The authors conclude that this proof-of-principle study identified candidate biomarker compounds linked with external gamma irradiation exposure and supports the hypothesis that breath VOCs may be employed for estimating exposures. Breath testing is rapid, non-invasive, and completely safe, and could be used potentially for estimating exposures in humans. This study employed laboratory-based instrumentation to analyze breath VOCs but could be successfully migrated to point-of-care platforms. A rapid and cost-effective point-of-care breath test using a mobile gas chromatograph accurately identified active pulmonary tuberculosis (Phillips et al. 2012). This was a preliminary study in a comparatively small number of animals; further studies will be required to validate the sensitivity and specificity of these candidate biomarkers, compare responses between species, definitively identify the biomarkers, and optimize the analytical instrumentation.

Acknowledgments—Michael Phillips is President and CEO of Menssana Research, Inc. This project was funded with Federal funds from the Biomedical Advanced Research and Development Authority, Office of the Assistant Secretary for Preparedness and Response, Office of the Secretary, Department of Health and Human Services, under Contract No. HHSO100201000010C.

REFERENCES

Arterbery VE, Pryor WA, Jiang L, Sehnert SS, Foster WM, Abrahams RA, Williams JR, Wharam MD, Risby TH. Breath ethane generation during clinical total body irradiation as a marker of oxygen-free-radical-mediated lipid peroxidation: a case study. Free Radical Biol Medicine 17: 569–576; 1994.

Barba CG, Calvo MM, Herraiz M, Santa-Maria G. Rapid detection of radiation-induced hydrocarbons in cooked ham. Meat Sci 90:697–700; 2012.

Chaudhry MA. Biomarkers for human radiation exposure. J Biomed Sci 15(5):557–563; 2008.

Cook NR. Statistical evaluation of prognostic versus diagnostic models: beyond the ROC curve. Clin Chem 54:17–23; 2008.

Crohns M, Saarelainen S, Laitinen J, Peltonen K, Alho H, Kellokumpu-Lehtinen P. Exhaled pentane as a possible marker for survival and lipid peroxidation during radiotherapy for lung cancer - a pilot study. Free Radical Research 43(10): 965–974; 2009.

de Oliveira CP, Nerin C, Rodriguez-Lafuente A, Soares Nde F. Multiple headspace-solid-phase microextraction as a powerful tool for the quantitative determination of volatile radiolysis products in a multilayer food packaging material sterilized with gamma-radiation. J Chromatography A 1244: 61–68; 2012.

Fedrigo M, Hoeschen C, Uwe O. Multidimensional statistical analysis of PTR-MS breath samples: a test study on irradiation detection. International J Mass Spectrom 295:13–20; 2010.

Forster R, Ancian P, Fredholm M, Simianer H, Whitelaw B. The minipig as a platform for new technologies in toxicology. Journal of Pharmacological and Toxicological Methods 62(3):227–235; 2010.

Guerrero T, Martinez J, McAleer MF, McCurdy MR, Wolski M. Elevation in exhaled nitric oxide predicts for radiation pneumonitis. International J Radiat Oncol Biol Phys 82:981–988; 2012.

Ismail HA, Lee EJ, Ko KY, Ahn DU. Fat content influences the color, lipid, oxidation, and volatiles of irradiated ground beef. Journal of Food Science 74(6):C432–C440; 2009.

Kim S, Koo I, Wei X, Zhang X. A method of finding optimal weight factors for compound identification in gas chromatography—mass spectrometry. Bioinformatics 28:1158–1163; 2012.

Kneepkens CM, Lepage G, Roy CC. The potential of the hydrocarbon breath test as a measure of lipid peroxidation. Free Radic Biol Med 17:127–160; 1994.

Li D, Wang Y, Wu H, Lu L, Zhang H, Chang J, Zhai Z, Zhang J, Zhou D, Meng A. Mitigation of ionizing radiation-induced bone marrow suppression by p38 inhibition and G-CSF administration. Journal of Radiation Research 52(6):712–716; 2011.

Ma S, Song X, Huang J. Regularized binomial ROC method in disease classification using microarray data. BMC Bioinformatics 7:253; 2006.

Marchetti F, Coleman MA. Candidate protein biodosimeters of human exposure to ionizing radiation. Int J of Rad Biol 82(9):605–639; 2006.

Moroni M, Prasanna PG. Triage dose assessment for partial-body exposure: dicentric analysis. Health Phys 98:244; 2010.

Moroni M, Coolbaugh TV. Hematopoietic radiation syndrome in the Göttingen minipig. Rad Res 176(1):89–101; 2011.

NCRP. Radiation dose reconstruction: principles and practices. Bethesda, MD: NCRP; Report No. 163; 2009.

Nam KC, Lee EJ, Ahn D, Kwon JH. Dose-dependent changes of chemical attributes in irradiated sausages. Meat Science 88(1):184–188; 2011.

Pass B. Collective radiation biodosimetry for dose reconstruction of acute accidental exposures: a review. Environmental Health Perspectives 105(Suppl 6):1397; 1997.

Phillips M, Cataneo RN, Cummin ARC, Gagliardi AJ, Gleeson K, Greenburg J, Maxfield FA, Rom WN. Detection of lung cancer with volatile markers in the breath. Chest 123(6): 2115–2123; 2003.

Phillips M, Basa-Dalay V, Bothamley G, Cataneo RN, Lam PK, Natividad MP, Schmitt P, Wai J. Breath biomarkers of active pulmonary tuberculosis. Tuberculosis 90(2):145–151; 2010.

Phillips M, Basa-Dalay V, Blais J, Bothamley G, Chaturvedi A, Modi KD, Pandya M, Natividad MPR, Patel U, Ramraje NN, Schmitt P, Udwadia ZF. Point-of-care breath test for biomarkers of active pulmonary tuberculosis. Tuberculosis (Edinburgh) 92:314–320; 2012.

Riley PA. Free radicals in biology: oxidative stress and the effects of ionizing radiation. Int J Radiat Biol 65:27–33; 1994.

Rosenfeld Y, Shai Y. Lipopolysaccharide (endotoxin)-host defense antibacterial peptides interactions: role in bacterial resistance and prevention of sepsis. Biochimica et Biophysica Acta 1758:1513–1522; 2006.

Stein S. Mass spectral reference libraries: an ever-expanding resource for chemical identification. Anal Chem 84: 7274–7282; 2012.

Viswanath L, Bindhu J, Krishnamurthy B, Suresh KP. Granulocyte-colony stimulating factor (G-CSF) accelerates healing of radiation induced moist desquamation of the skin. Klinicka Onkologie: Casopis Ceske a Slovenske Onkologicke Spolecnosti 25(3):551–560; 2008.

Wang B, Fang A, Heim J, Bogdanov B, Pugh S, Libardoni M, Zhang X. DISCO: distance and spectrum correlation optimization alignment for two dimensional gas chromatography time-of-flight mass spectrometry-based metabolomics. Analytical Chemistry 82:5069–5081; 2010.

Wilkins RC, Romm H, Kao TC, Awa AA, Yoshida MA, Livingston GK, Jenkins MS, Oestreicher U, Pellmar TC, Prasanna PG. Interlaboratory comparison of the dicentric chromosome assay for radiation biodosimetry in mass casualty events. Rad Research 169(5):551–560; 2008.

Yang J, Zhu J, Zou YY. A robust statistical procedure to discover expression biomarkers using microarray genomic expression data. J Zhejiang Univ Sci B 7:603–607; 2006.

Zhu MJ, Mendonca A, Lee EJ, Ahn DU. Influence of irradiation and storage on the quality of ready-to-eat turkey breast rolls. Poultry Science 83(8):1462–1466; 2004.

■■